H^+-Pumping Rhodopsin from the Marine Alga *Acetabularia*

Satoshi P. Tsunoda,* David Ewers,† Sabrina Gazzarrini,‡ Anna Moroni,‡ Dietrich Gradmann,† and Peter Hegemann*

*Experimentelle Biophysik, Fachbereich für Biologie, Humboldt-Universität zu Berlin, 10115 Berlin, Germany; †A.-v.-Haller-Institut der Universität, 37073 Göttingen, Germany; and ‡Dipartimento di Biologia and Consiglio Nazionale delle Ricerche Istituto di Biofisica, Università degli Studi di Milano, 20133 Milan, Italy

ABSTRACT An opsin-encoding cDNA was cloned from the marine alga *Acetabularia acetabulum*. The cDNA was expressed in *Xenopus* oocytes into functional *Acetabularia* rhodopsin (AR) mediating H^+ carried outward photocurrents of up to 1.2 μA with an action spectrum maximum at 518 nm (AR_{518}). AR is the first ion-pumping rhodopsin found in a plant organism. Steady-state photocurrents of AR are always positive and rise sigmoidally from negative to positive transmembrane voltages. Numerous kinetic details (amplitudes and time constants), including voltage-dependent recovery of the dark state after light-off, are documented with respect to their sensitivities to light, internal and external pH, and the transmembrane voltage. The results are analyzed by enzyme kinetic formalisms using a simplified version of the known photocycle of bacteriorhodopsin (BR). Blue-light causes a shunt of the photocycle under H^+ reuptake from the extracellular side. Similarities and differences of AR with BR are pointed out. This detailed electrophysiological characterization highlights voltage dependencies in catalytic membrane processes of this eukaryotic, H^+-pumping rhodopsin and of microbial-type rhodopsins in general.

INTRODUCTION

In 1968, Schilde (1) reported a fast, light-induced response of the transmembrane voltage from the giant unicellular marine alga *Acetabularia acetabulum* (former *A. mediterranea*; Fig. 1 *A*) and suggested rhodopsin to be the responsible photoreceptor, long before any other rhodopsin was found outside the animal kingdom. The observation has been interpreted by an inhibition of a Cl^--importing ATPase (2,3). However, several attempts to isolate this Cl^--ATPase failed because of the wrong substrate (only an H^+ ATPase was found (4)) or the wrong genetic code (5), which differs in *Acetabularia* from normal (6).

Recently, Mandoli and co-workers (7) reported a cDNA sequence from juvenile *Acetabularia* (Fig. 1 *A*) as a fragment of a tentatively opsin-encoding gene (Acetabulariaopsin, *aop*). Opsins are membrane-spanning proteins that covalently bind retinal as a chromophoric light-absorbing cofactor thus forming the functional photoreceptor *rhodopsin*. Three rhodopsin classes can be distinguished according to their electrical properties: i), Electrically neutral rhodopsins operate as visual photoreceptors in animal eyes or sensors for phototaxis in prokaryotes; ii), light-driven ion pumps for H^+ and Cl^- form a primordial mechanism of photosynthetic energy conversion in archaea and eubacteria (8–11); and iii), channel rhodopsins from phototactic algae mediate light-induced passive conductance of H^+ and other cations (12,13).

The best-characterized rhodopsin is the proton-pumping bacteriorhodopsin (BR) from *Halobacterium salinarium*. A simplified reaction scheme of the H^+-pumping process according to Luecke et al. (14) is shown in Fig. 1 *B*. In this scheme, the retinal Schiff base (S) is represented in two conformations, S_i and S_o, with H^+ accessibility either from the internal medium or the external bulk phase, respectively. In darkness, the Schiff base is protonated, and its H^+ binding site faces the extracellular bulk phase. The Asp serving as internal H^+ donor is protonated, D_iH, and the Asp serving as H^+ acceptor unprotonated, D_o. During the photocycle S_oH transfers the H^+ to D_o. S_o undergoes a conformational switch to S_i and is reprotonated by D_i. Then S_iH reisomerizes to S_oH. All intermediate steps have been characterized by numerous spectroscopic measurements (ultraviolet/Vis, Fourier transform infrared spectroscopy, and resonance Raman spectroscopy), and the three-dimensional structure is known from most photocycle intermediates. However, the photocycle of isolated rhodopsin has never been analyzed in detail at negative membrane voltage, where it operates under natural conditions, and only very little is known about the separate roles of internal and external pH. Previous electrophysiological studies of pumping rhodopsins (15,16) presented rather linear current-voltage relationships, *I*/*E*, and the authors applied linear models for the analysis correspondingly. This approach yielded puzzling intersections of the extrapolated *I*/*E* relationships with the voltage axis. It also resulted in nonsaturating kinetics colliding with the expected properties of an H^+-pumping enzyme.

We cloned a full-length *opsin*-cDNA from *Acetabularia*, expressed it in *Xenopus* oocytes, and studied the properties of the corresponding rhodopsin, *Acetabularia* rhodopsin (AR), by voltage-clamp techniques. During this study, AR

Submitted April 3, 2006, and accepted for publication May 18, 2006.

Satoshi P. Tsunoda and David Ewers contributed equally to this work.

Address reprint requests to Dietrich Gradmann, Tel.: 49-7071-550005; Fax: 49-7071-869001; E-mail: dgradma@uni-goettingen.de.

David Ewers's present address is Abteilung Neurophysiologie, Medizinische Hochschule Hannover, Carl-Neuberg-Strasse 1, 30625 Hannover, Germany.

0006-3495/06/08/1471/09 $2.00

doi: 10.1529/biophysj.106.086421

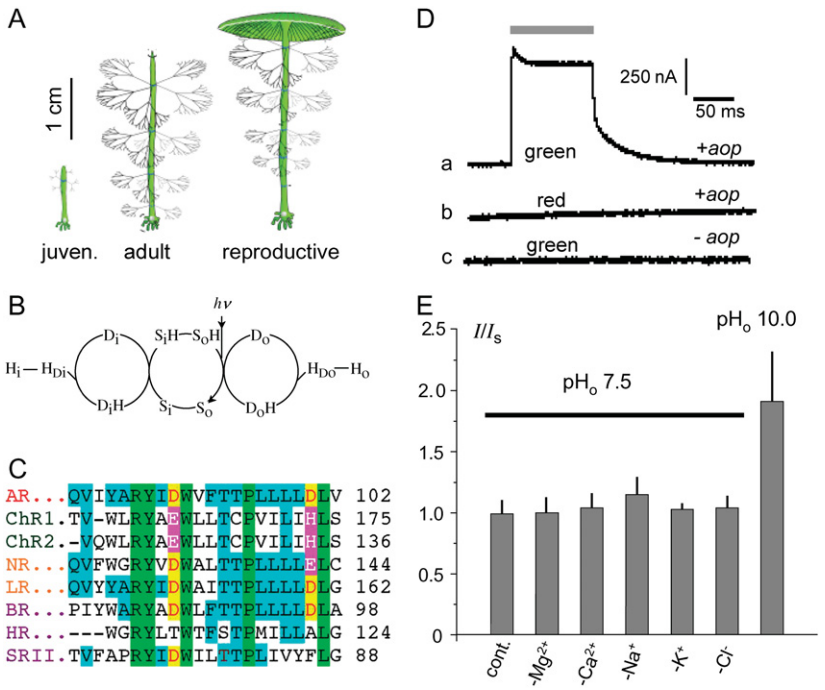

FIGURE 1 Basic relationships. (*A*) Sketched cells of *A. acetabulum* in three developmental states, modified from Henry et al. (7). (*B*) Hypothetical reaction scheme for light-driven H^+ export through BR and AR. Due to structural analogies in AR and BR (Fig. 1 *B* and Supplement-1), we define D_i: D-100 in AR and D-96 in BR (H^+ donor), D_o: D-89 in AR and D-85 in BR (H^+ acceptor); $S_i(_o)$: Schiff base with H^+-binding site facing internal (external) bulk phase; protonated and deprotonated states as marked. H_i: cytoplasmic $[H^+]$; H_{Di}: $[H^+]$ at entry of reaction cycle; H_{Do}: $[H^+]$ at release site from reaction cycle, H_o: lumenal $[H^+]$. (*C*) Comparison of microbial rhodopsin amino acid sequences in the range of helix 3. The top four eukaryotic sequences are AR (AR DQ074124), ChR1 (Channel rhodopsin-1, AF385748), ChR2 (Channel rhodopsin-2, AF461397) both from *Chlamydomonas reinhardtii*, NR (Neurospora rhodopsin AF, XM_95432) from *Neurospora crassa*, LR (Leptosphaeria rhodopsinAF290180) from *Leptosphaeria maculans*, followed by BR (BR, AAA72504), HR (halorhodopsin, CAB3786), and SRII (sensory rhodopsin II, P42196) all from *Halobacterium salinarium*. Lettering: green: algae, yellow: fungi, violet: archaea. Amino acids identical in all sequences are underlayed in green, identical in AR and some others are in blue, H^+-donor and acceptor groups in yellow and functional substitutes of these in violet. (*D*) Basic observations of photocurrents from AR expressing *Xenopus* oocytes, bathed in ND-96 solution pH 7.5, holding voltage 40 mV; top bar: light period; *a–c*: conditions as marked; green light: peak at 500 nm, *J* 100%; red light: $\lambda > 600$ nm ($J > 10^{23}$ photons m^{-2} s^{-1}). (*E*) Depletion of major ion species in bath has no effect on steady-state photocurrents at +40 mV and 100% green light, except H^+.

turned out to be a light-driven H^+ exporting pump. Most properties of AR are similar to those of BR from *H. salinarium* (14), but the sensitivities of AR to pH and voltage differ considerably from those reported from BR. The sigmoid *I/E* relationships described here allow a straightforward enzyme kinetic interpretation of the results.

MATERIALS AND METHODS

Plant material

Axenic cultures of *A. acetabulum* were obtained according to Schweiger et al. (17) in Müller's medium (18) at 20°C and a light:dark cycle of 14:10 h, 10–12-mm long, about 3-week-old cells were harvested immediately after a dark period of 16 h, weighed and washed with Müller's medium, shock frozen in liquid nitrogen, and stored at −80°C.

RNA isolation

The frozen cells were ground in a mortar with a pestle under liquid nitrogen. The powder was suspended in extraction buffer (100 mM LiCl, 100 mM Tris/HCl, pH 8.0, 10 mM EDTA, 1% β-mercaptoethanol) at a ratio of 1:3 (w/v), followed by an extraction once with phenol-chloroform and once with chloroform. A solution of 8 M LiCl was added to the aqueous phase at a ratio of 1:3 (v/v) and the mixture was stored overnight at 4°C. The precipitate was pelleted (12,000 × *g*, 10 min) and washed with 2 M LiCl, then with 70% ethanol. The pellet was solved in 0.1% diethylpyrocarbonate-treated, sterilized H_2O.

RACE

Total RNA was reverse transcribed using RevertAid H Minus First Strand cDNA Synthesis Kit (MBI-Fermentas, St. Leon-Rot, Germany) with 2 mg of total RNA and 2.5 mM of a $(dT)_{16}$ primer under the conditions recommended by the manufacturer. Polymerase chain reaction (PCR) was performed on the cDNA with a gene-specific primer (5′CGGATGAGCGTGAAGTTA3′) and the oligo(dT) primer to amplify the 3′-end of the putative *Acetabularia* opsin (7) that has the Genbank accession No. CF259014. For 5′-RACE, cDNA was generated as described for the 3′-RACE, except that 1 mM of a gene-specific primer (5′GCACGGCAAGCATGATGCAGCCGAC3′) was used instead of oligo(dT) primer. The cDNA was poly dG tailed with terminal nucleotide transferase (MBI-Fermentas), according to the suppliers instructions. PCR was carried out using a poly dG-specific primer (5′$T(C)_{15}$3′) and a nested gene-specific primer (5′CCGTCGACGGTGAATGCGCCGATGATAC3′). The amplicons were sequenced (SEQLAB, Göttingen, Germany).

Generation and cloning of full-length *aop*

The full-length sequence was amplified in a PCR with two primers derived from the sequences obtained by 3′-RACE (5′AGTCTAGAAAGGATGCTTGCAATATCA3′, introducing an XbaI restriction site) and 5′-RACE (5′ACCTGCAGATCTCACGTTCTGTA3′, introducing a PstI restriction site). The product was cut with XbaI/PstI and ligated into a XbaI/PstI cut pUC19 plasmid (MBI-Fermentas). The sequence of the 1027 bp insert can be found under the Genbank accession no. DQ074124.

Mutagenesis and cloning for heterologous expression

To take differences concerning the genetic code (6) into account, *aop* was mutagenized through the megaprimer method (19) following the protocol provided by Tyagi et al. (20). The mutagenic primer (5′CGGCCGGAACTGAACAGCGATGGAA3′, antisense) was designed to replace a stop codon (TAA (STOP) changed to CAG (Q)), the first flanking primer (5′CGCGGATCCATGTCAAACCCTAACCCT3′, sense) introduced a *Bam*HI restriction

site, and the second flanking primer (5′TTCAAGCTTCCTCGAGCCCC-AACTTTTCC3′, antisense) introduced an *Xho*I restriction site. The first PCR mixture contained 20 nM of the mutagenic primer, 1 nM of the first flanking primer, and 100 ng of pUC19-*aop* DNA. Before initiation of the second round of PCR, second flanking primer was added to a concentration of 20 nM. PfuUltra Hotstart DNA Polymerase (Stratagene, Amsterdam, The Netherlands) was used instead of Vent Polymerase. *Aop*mut was cut with *Bam*HI/*Xho*I and ligated into the polylinker of pSGEM (courtesy of M. Hollmann, Max Planck Institute for Experimental Medicine, Göttingen, Germany).

Heterologous expression in *Xenopus* oocytes

A full-length cRNA, $AR_{1–279}$ (aa 1–279), and a truncated version, $AR_{1–235}$ (aa 1–235), were synthesized in vitro from NsiI-linearized *aop*-pSGEM plasmid by using T7 RNA polymerase (Riboprobe system T7, Promega, Mannheim, Germany). Because the transport properties of both were qualitatively indistinguishable, most experiments were carried out with $AR_{1–235}$. Oocytes were prepared from female *Xenopus* as described previously (21), then single oocytes were injected with 50 nl of water or 50 nl of *aop*-cRNA (0.5 μg/μl) and incubated in the dark at 19°C in oocyte ringer solution (96 mM NaCl, 2 mM KCl, 1.8 mM $CaCl_2$, 1 mM $MgCl_2$, 5 mM MOPS (3-(*N*-morpholino)propanesulfonic acid), adjusted to pH 7.5 with NaOH) in the presence of 5 mM Na-pyruvate and 50 μg/ml gentamicin and in the presence of 1 μM all-*trans*-retinal (SIGMA, Taufkirchen, Germany). Interestingly, retinal addition turned out to be unnecessary. In contrast to BR (16) and channel rhodopsin (12) the affinity of AR for retinal appears so high that complete reconstitution occurs with endogenous retinal. Measurements were performed 3–7 days after injection.

Electrophysiology

Two-electrode voltage clamp was performed to record photocurrent of AR on *Xenopus laevis* oocytes using a GeneClamp 500 amplifier (Axon Instruments, Union City, CA) and Turbo Tec-03X (NPI Electronic, Tamm, Germany). Data acquisition and light triggering were controlled with pCLAMP 9.0 software via DigiData 1322A interface (Axon Instruments). The temporal resolution of the recording system was ~1 ms. The data obtained were normally averages of three runs. The microelectrodes were fabricated by pulling borosilicate glass capillaries (1.50 mm o.d. and 1.17 mm i.d.) using a micropipette puller (model P-97, Sutter instrument, Novato, CA) and filled with 3 M KCl. The resistances of microelectrodes were 0.5–1.5 MΩ. A 75-W xenon lamp (Jena-Instruments, Jena, Germany) was used for the source of green (500 nm) or red (600 nm) light. The light was applied to the oocytes by using a 2-mm light guide. Green light at 100% (K50 filter, Balzers Liechtenstein) corresponds to 1.5×10^{22} photons s^{-1} m^{-2} at the surface of the oocyte. For the blue-light experiment (405 nm), a CUBE 405 laser system (Coherent, Dieburg, Germany) was employed. Blue light at 100% corresponds to 3.1×10^{21} photons s^{-1} m^{-2}. Lowering of pH_i was accomplished by exposure to butarate, following the protocol for pH_i changes in *Xenopus* oocytes (22).

RESULTS

Basic observations

The partial sequence of the opsin-related cDNA already sequenced by Mandoli and co-workers (7) contained the fragment encoding helix 3 (Fig. 1 *C*). This helix comprises the two aspartates, D-89 and D-100, that in BR function as primary donors, D_i, and acceptors, D_o, of the Schiff base proton during the photocycle. Since the donor D-100 (D-96 in BR) is conserved in H^+-pumping rhodopsins but is absent in anion transporters, sensors, and channel rhodopsins, it was likely that the identified cDNA encodes an H^+-transporting protein.

RNA was isolated from juvenile, ~20-day-old *Acetabularia* cells. The complete cDNA was isolated and sequenced. The derived 279 amino acid protein comprising seven hypothetical membrane-spanning domains belongs to the microbial-type rhodopsin family with the most striking homology to BR. Within this new AR besides the hypothetical retinal binding Lys, K-218, most amino acids forming the proton transporting hydrogen network in BR are also conserved, namely, Y-60, R-86, Y-87, D-89, D-100, E-206, and D-214 (shown in *red* in Fig. 1 *C* and Supplement-1), corresponding in BR to Y-57, R-82, Y-83, D-85, D-96, E-204, and D-212 (14). A-195 and G-196 in AR surprised us since the respective S-193 and E-194 in BR are involved in the extracellular H^+ release, although these amino acids are also not conserved in the fungal proton-pumping rhodopsin from *Leptosphera* (11) either.

RNA encoding either the full-length AR ($AR_{1–279}$) or a shorter version covering amino acid 1–235 ($AR_{1–235}$) were prepared and injected into *Xenopus* oocytes. Between 3 and 7 days after RNA injection, strong green light caused striking outward currents (Fig. 1 *Da*), whereas red light of similar intensity did not (Fig. 1 *Db*). Oocytes injected with RNA-free water did not show any light response either (Fig. 1 *Dc*). This was the first evidence that AR is a green-light-driven transport protein. Since oocytes expressing $AR_{1–235}$ showed photocurrents with similar kinetics but larger amplitudes than those expressing $AR_{1–279}$, all further experiments were carried out with $AR_{1–235}$.

To identify the transported ion species, cations and anions of the medium were exchanged or omitted, i.e., Cl^- was exchanged for aspartate, Na^+ for *N*-methyl-D-glucosamine, and Ca^{2+} was simply left out. In none of these experiments (three per ion species) did the current change significantly (Fig. 1 *E*), suggesting that none of these ions is transported by AR. However, depletion of extracellular H^+ stimulated the photocurrents (pH_o 10 in Fig. 1 *D*).

The light/response relationships of AR (example in Fig. 2 *A*) show saturation kinetics like ordinary enzymes, which can be linearized by double-reciprocal plots (Fig. 2 *B*), at least for high light intensities. This evaluation yielded a high half-saturating light intensity especially for pH_o 10, indicating a fast photocycle that is enhanced at pH 10. Interestingly, the two linear relationships in Fig. 2 *B* are parallel. Kinetically this is treated as ''uncompetitive inhibition,'' which means the inhibitor is binding to the enzyme substrate complex inhibiting substrate release. Stimulation is expected at high pH_o for unidirectional H^+ export through an acceptor (D_o) that is equilibrating rapidly with the external medium (theoretical reasoning in Supplement-2). Deprotonation of D_oH is inhibited at low pH.

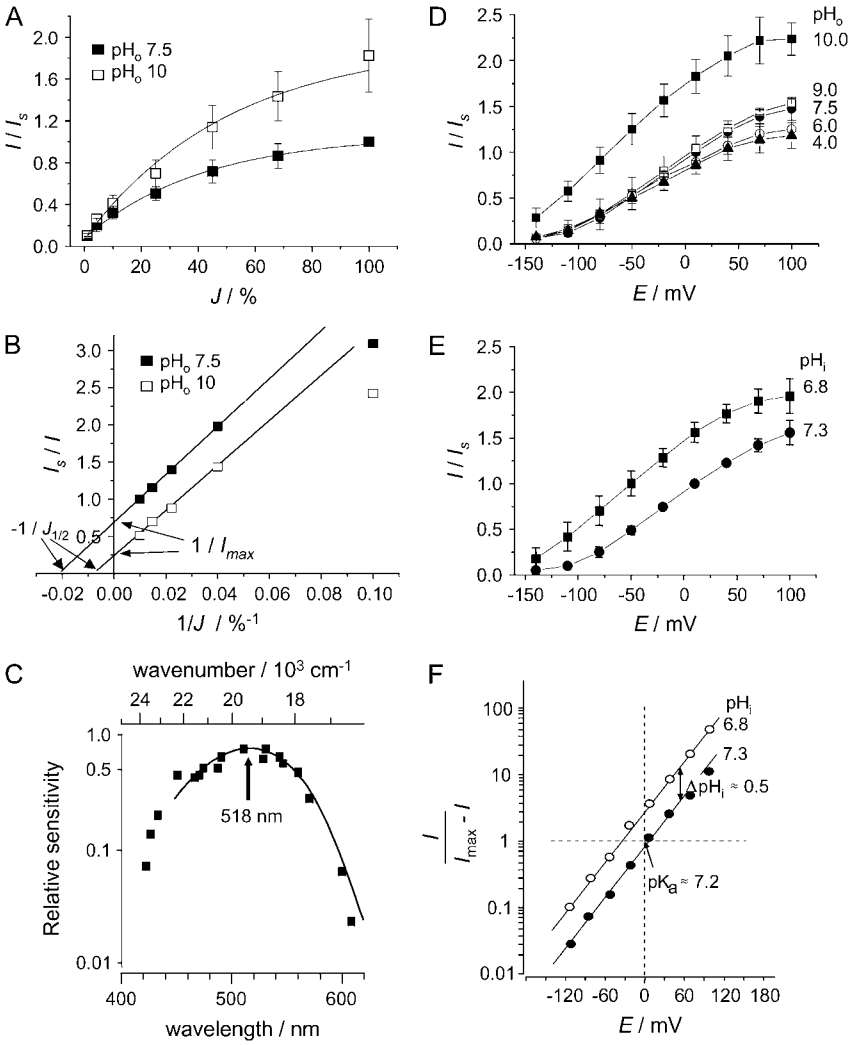

FIGURE 2 Light- and pH-sensitivity of steady-state photocurrents. (*A*) Typical light/response relationship, recorded with 500-nm light at +40 mV, pH_o 7.5 (control) and pH_o 10. Standard current, $I_S = 67.7 \pm 9.3$ nA ($n = 8$) at pH_o 7.5. and 100% *J*. (*B*) Same data as in *A* in double-reciprocal plot. (*C*) Action spectrum constructed from light/response relationships (reciprocal half-saturation intensities), recorded at different wavelengths. (*D*) Effect of pH_o on steady-state *I*/*E* relationships in 100% light; data normalized to standard photocurrent, $I_S = 61.6 \pm 7.8$ nA ($n = 15$) at 0 mV and pH_o 7.5. After each measurement, cells were exposed to the reference medium to avoid pH_i changes. (*E*) Effect of pH_i on steady-state *I*/*E* relationships in 100% light; data normalized to I_S as in Fig. 2 *D*. (*F*) Same data as in panel *E*, replotted as $\log(I/(I_{max} - I))$; linear relationship equivalent to Hill plot in ordinary enzyme kinetics; difference between pH_i 6.8 and pH_i 7.3: parallel vertical shift by half a log unit per $\Delta pH_i = 0.5$; pH_i-insensitive slope: ≈0.6 log units (factor $10^{0.6} = 4$) per 60 mV.

From light/response curves recorded at different wavelengths, an action spectrum was constructed (Fig. 2 *C*). It is rhodopsin shaped, peaking at $\lambda = 518$ nm, i.e., blue-shifted by ~30 nm compared to the spectrum for the fast depolarization in *Acetabularia* (1–3). This discrepancy may be explained by the different molecular environment of AR in native and heterologous membranes.

Sensitivity of steady-state photocurrent to voltage, pH_o, and pH_i

The sensitivity of the photocurrents to the chemical and electrical terms of the proton motive force was studied by measuring the steady-state photocurrents under variation of the membrane voltage, the external pH (pH_o), and the internal pH (pH_i). The steady-state photocurrents are always positive and rise sigmoidally from small values at very negative voltages to saturation in the positive voltage range. Fig. 2 *D* shows that varying pH_o between 4 and 9 changes the photocurrent very little, especially in the negative voltage range. However, at pH_o 10 the current is significantly increased over the whole voltage range, indicating that the rate-limiting proton release group has a $pK_a > 9$. In contrast, changing pH_i by only half a unit causes a considerable increase of the currents already in the neutral pH range (Fig. 2 *E*). Considering AR as an enzyme with internal H^+ as substrate we may apply the Hill formalism:

$$I = I_{max}\frac{H_i^n}{K_m + H_i^n} \quad (1)$$

or after rearranging

$$\log\frac{I}{I_{max} - I} = n\log H_i - \log K_m = pK_a - npH_i. \quad (2)$$

Thus, plotting $\log(I/(I_{max} - I))$ versus $-\log H_i$ (i.e., pH_i) would result in a straight line with the slope n. For a demonstration of the equivalence of pH_i and voltage changes that are sensed by the proton donor group D_i, we distinguish the H^+ concentration in the cytoplasm, H_i, from the H^+ concentration at the donor site, H_{Di} (on a molecular level

better described as an H^+ occupation probability). Defining d_iE as the voltage fraction that drops over the internal H^+ access channel, IC, we get

$$d_iE = 2.3\frac{RT}{F}\cdot\log\frac{H_i}{H_{Di}} = 59\,\text{mV}\cdot(pH_i - pH_{Di}). \quad (3)$$

Substituting pH_i in Eq. 2 by $pH_{Di} = pH_i - (d_iE/59\ \text{mV})$ yields

$$\log\frac{I}{I_{max}-I} = pK_a - pH_i + \frac{d_iE}{59\,\text{mV}}. \quad (4)$$

Replotting of the data from Fig. 2 *E* to Fig. 2 *F* in this way yields parallel linear relationships with the slope of 0.6 and a vertical distance of ~0.5 log units, which exactly reflects the different pH_i conditions applied. The slope of ~0.6 log units per 60 mV means that ~60% of the applied voltage causes apparent changes of pK_a of D_i, Correspondingly, the pH_i 6.8 relationship crosses the $E = 0$ line at ~0.4 log units above the origin, yielding the same $pK_a = pH_i + 0.4 = 7.2$ for the H^+-binding site D_i.

Dynamics

Fig. 3 *A* shows original photocurrent records from one oocyte clamped at different holding voltages E_h between −110 and +70 mV. In general, the temporal response upon rectangular light-on stimulation comprises a transient and a stationary component: upon light-on, there is a fast response, *a*, that relaxes to the stationary level with the time constant τ_1. Since the rise of *a* is faster than the resolution of our detection system, the recorded peaks are underestimates of the true *a*. Upon light-off, the current relaxation to zero also has a fast component, *b*–*c*, and a slow component, *c*, with the time constants τ_2 and τ_3, respectively. The fast one is again not resolved. The voltage sensitivities of the three amplitudes *a*, *b*, and *c* are similar (Fig. 3 *B*).

The time constant τ_1 is virtually voltage independent, whereas τ_3 shows a constant voltage dependence (Fig. 3 *C*). The more positive the voltage, the faster the current relaxation after light-off. Since the amplitude *c* also rises with more positive voltages, the integral $Q = \int c\,dt = c\tau_3$ turns out to be rather constant around 10 nAs over a considerable voltage range.

Detailed light/response relationships

The basic light/response relationship of the steady-state photocurrent *b* is already presented in Fig. 2, *A* and *B*. Now, we focus on the dependence of the individual kinetic phenomena on the light intensity. Fig. 4, *A*–*F*, shows examples of photocurrent records upon light pulses of different intensity at two voltages. The general observation is that *b* saturates faster than *a* with increasing light. This relationship results in initial current peaks with large amplitudes at higher light intensities. Since the steady-state currents are larger at positive voltage, transient peaks are less pronounced (Fig. 4) in this voltage range, especially at low light.

The amplitudes *b* and *c* change in parallel to changes in voltage (Fig. 3 *B*) and/or light (visible in Fig. 4, *A*–*C*; $b{:}c \approx 3$) throughout. The half-saturating light intensity ($J_{1/2}$, determined by the marked intersection of the inverted intensity curve with the abscissa) is not influenced by the voltage

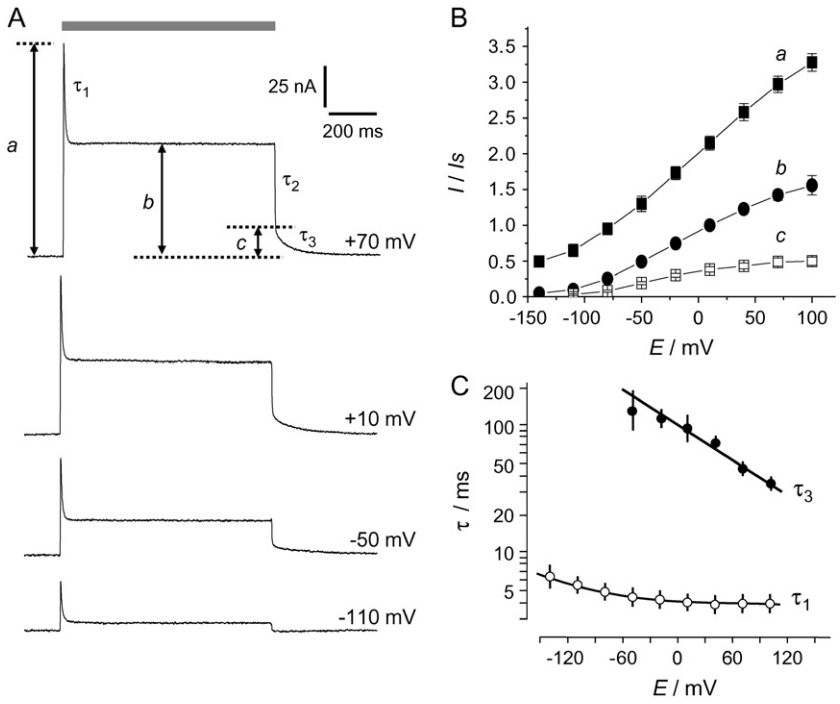

FIGURE 3 Voltage sensitivity of amplitudes and time constants of photocurrents. (*A*) Four individual current traces recorded at different voltages at pH_o 7.5. (*B*) Amplitudes of *a* (instantaneous current), *b* (steady-state current), and *c* (slowly decaying current component after light-off) plotted versus voltage. Means ± SE from seven cells, normalized to *b* at 0 mV, and reference pH conditions (pH_i 7.3, pH_o 7.5); (*C*) τ_1 and τ_3 plotted logarithmically versus voltage; note rather constant $Q = \tau_3 c \approx 10$ nAs over a wide voltage range, i.e., (in nAs): 6.8 at −70 mV, 8.8 at −40 mV, 11 at −10 mV, 12 at 20 mV, 12 at 50 mV, and 8.9 at 80 mV.

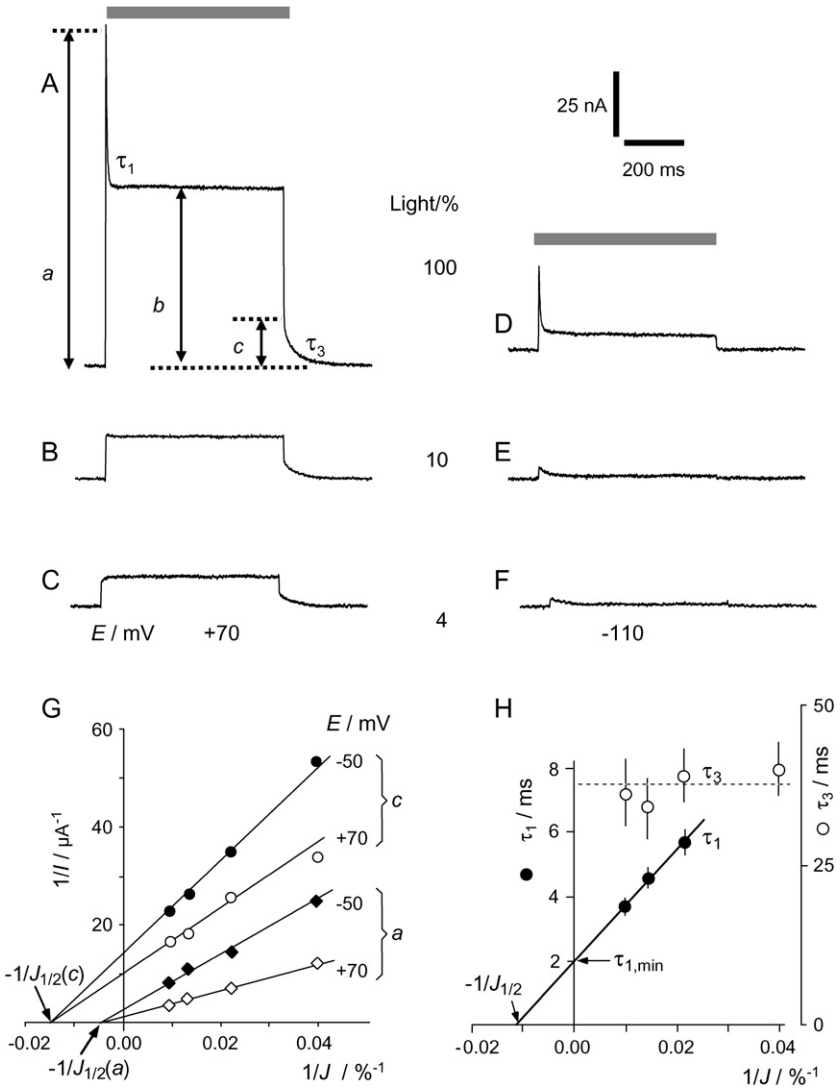

FIGURE 4 Intensity sensitivities of the individual dynamic components in AR photocurrents. (*A–F*) Example records (pH_o 7.5) at different light intensities at +70 and −110 mV. (*G*) Double-reciprocal plots of light/response relationships of photocurrents *a* and *c* (defined in panel *A*) at +70 and −110 mV; for *b* relations, see Fig. 2 *B*; note voltage-insensitive $J_{1/2}$. (*H*) Time constants τ_1 and τ_3 versus $1/J$, corresponding to double-reciprocal plots of transition probabilities $k = 1/\tau$ versus J.

(Fig. 4 *G*) and is larger for *a* than for *c* and *b*, correspondingly. The time constant τ_1 describes the decrease of the photocurrent from the initial value to the steady-state level *b*. This time constant decreases down to 2 ms with increasing light intensities (Fig. 4 *H*). It reflects the depletion of S_oH (AR_{518}). In contrast, τ_3 reflects a dark process and thus shows no obvious light dependence (Fig. 4 *H*).

Double pulse experiments

When two bright light pulses are applied, separated by a short dark interval, the second transient current was smaller than the one evoked by the first pulse, whereas the steady-state level remained constant (Fig. 5, *A–D*). This refractory behavior was weak at positive (Fig. 5, *A* and *B*) and more pronounced at negative voltages (Fig. 5, *C* and *D*). The resulting time constants τ_4 for recovery of the dark state are derived from the recoveries of the full size transient current at all voltages in Fig. 5 *E* and listed in the inset. In comparison with τ_3, τ_4 has about the same voltage sensitivity (approximately twofold faster recovery per +60 mV), but the underlying process is ~3 times slower throughout.

Probing for the blue-light-absorbing photocycle intermediate

Since it was likely that τ_3 reflects the reprotonation of the retinal Schiff base, we probed for a blue-shifted photocycle intermediate by application of blue light pulses of 405 nm on top of strong green light exposure. The results in Fig. 5 *F* show a short current transient upon blue-light-on, followed by a continuous reduction of the green-light-mediated outward current. Both the fast and the slow response on blue-light always appear negative and voltage independent. The reduction of the steady-state current is ~30% smaller in pH_o 10 compared to pH_o 7.5 (data not illustrated), indicating less accumulation of M-intermediates at pH_o 10.

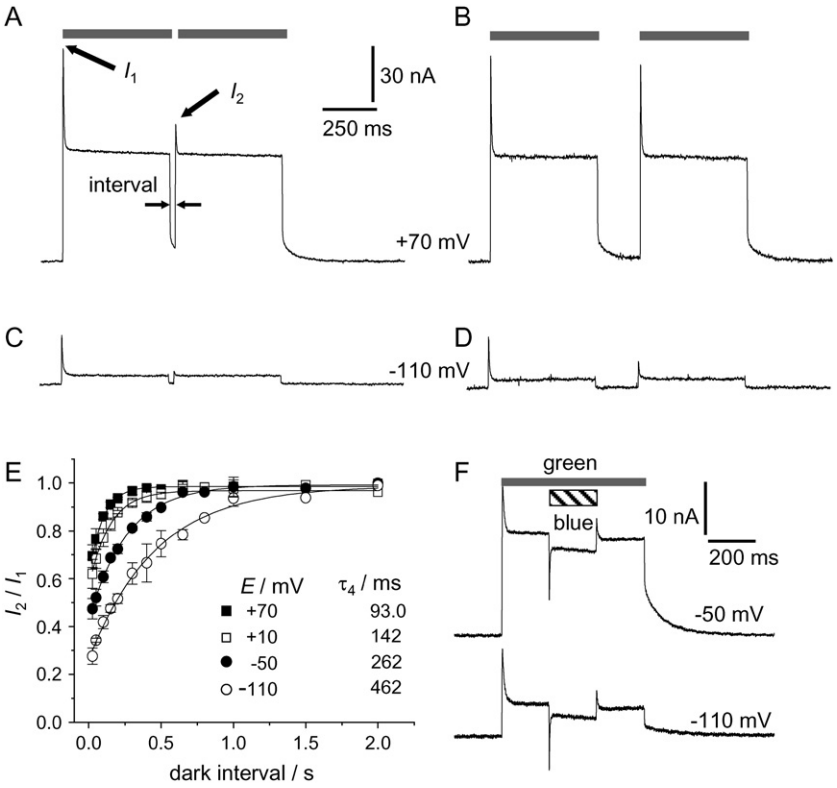

FIGURE 5 Kinetic recovery after illumination. (*A–D*) Example records of exposure to a second light pulse after a reference light pulse (100% intensity) and dark periods of various durations, recorded at +70 mV and −110 mV as marked. (*E*) Systematic evaluation of experiments like *A–D*: Exponential recovery (means ± SE, $n = 4$) of response *b–a* (s. Fig. 4 *A*) during dark period with τ_4, faster at positive and slower at negative voltage; compare Fig. 3 *C*, and notice $\tau_4 > \tau_3$. (*F*) Effect of blue-light ($\sim 10^{22}$ photons m^{-2} s^{-1}, 500 nm, generated by blue-light laser) on standard, green-light induced steady-state photocurrents (100% *J*, pH_o 7.5), at −50 and −110 mV; blue-light-on: fast negative transient followed by continuous reduction of positive steady-state current; blue-light-off: qualitatively symmetric response with fast, positive transient, followed by steady-state level; note: the blue-light response is independent of the voltage.

DISCUSSION

General aspects

AR is an additional member in the new and short list of BR-like rhodopsins in eukaryotes (10,11), one of the only two known H^+-pumping rhodopsins from eukaryotes and the first reported proton-pumping rhodopsin from a photosynthetic eukaryote. It can be excluded that the AR-cDNA (*aop*) belongs to a contaminating organism since the *aop* encodes a rhodopsin in *Xenopus* only after changing the unusual genetic code of *Acetabularia* (6) into normal. Common features of the photoelectric response in *Acetabularia* (1–3) and of AR comprise the similar action spectrum, the rapid onset of the light-induced current, the high light intensity for half-saturating response, and the low sensitivity to pH_o between pH_o 9 and pH_o 4. Because of these similarities we might assume that AR is the photoreceptor of the fast photoelectric response in *Acetabularia*. However, it is puzzling that the fast photoelectric response is an inward current, whereas the green-light-induced currents of AR described here are outward currents throughout. Thus, it would be premature here to speculate about the physiological role of AR in *Acetabularia*. Possibly, the behavior of the heterologously expressed AR differs from its in vivo function.

Functional comparison with BR

The similar shape of the photocurrents with transient and stationary components and the high half-saturating intensity indicate strong similarities between AR and BR. Significant kinetic differences between AR and BR exist with respect to sensitivity to pH_i and pH_o. Characteristic of AR is a high sensitivity to pH_i (Fig. 2 *E*) and a low sensitivity to pH_o (Fig. 3 *D*). For BR, a strong, straightforward dependence on the substrate concentration is only reported when D_i is mutated into a nonacidic group, D96N (23). In contrast, AR shows no pH_i-shielding influence of D_i, as shown by the pH_i-induced difference of the normalized current $I/(I_{max} - I)$ by exactly 1 log unit per ΔpH_i (Fig. 2 *F*).

The photocurrents of AR show virtually no pH_o sensitivity between pH_o 4 and 9, whereas those of BR are ~10% reduced per pH_o unit at 0 mV and $pH_o < 7.5$ (16). This weak pH_o sensitivity of both AR and BR is explained by the H^+-shielding effect of the H^+ pathway (24) between S_oH and the external bulk solution. For $pH_o > 9$, only the photocurrents from AR (presented here) are available. They show a significant stimulation at pH_o 10 at all voltages (Fig. 2 *D*). This means, only when the external proton concentration is very low ($pH_o > pK_a \approx 9$) is the D_o group rapidly deprotonated after retinal reisomerization from 13-*cis* to 13-*trans* (25). This interpretation agrees with the finding that the apparent pK_a of the D_o group changes from a very low value (~3) in the all-*trans* conformation of the ground state to a very high value (~11) in the 13-*cis* conformation (14). It might be surprising that the enhancement at $pH_o > 9$ is seen even at negative voltage, when H^+ uptake should be rate limiting. This phenomenon is explained by the connectivity model in which all intermediates L, M1, M2, and N are

in equilibrium as long as the retinal is in the 13-*cis* conformation (25).

The steepness of the sigmoid *I*/*E* relationship may be expressed by the voltage interval between 10% and 90% saturation. In comparison to BR, where approximate linearity of *I*/*E* has been reported between −150 and +50 mV (16), the sigmoid *I*/*E* relationships of the photocurrents of AR in this voltage range (e.g., Fig. 2, *D* and *E*) indicate that the limiting reaction steps of the reaction cycle of AR sense a larger fraction of the total voltage than in BR.

Number of excited molecules

One striking relationship in the results of Fig. 3 is the rather constant and voltage-independent current integral $Q = \tau_3 c \approx$ 10 nA s after light-off. These 10 nAs ($\tau_3 c$) correspond to $n =$ $Q/e \approx 6 \times 10^7$ elementary charges, possibly reprotonating S_i into S_iH (Fig. 3 *C*). Thus, the number of charges transported after the light-off (at high light intensities) is more or less voltage independent, which is consistent with the voltage insensitivity of the blue light response. Anticipating that 40% of the charge is transported in the slow part of the photocycle, this number corresponds to $N = 2.5 \times Q/e =$ 1.5×10^8 AR molecules at 50% *J*. Accordingly, the total number of functional rhodopsins is $\sim 3 \times 10^8$ molecules in the oocyte membrane.

Rate limitation

The slowest step in the reaction cycle (τ_4) reflects the recovery of the full AR sensitivity. It is pH_o and voltage sensitive and extremely slow at negative voltage and acidic pH_o. Since for the BR photocycle, deprotonation of D_oH (Fig. 1 *B*) is accepted as the slowest reaction at low pH_o (O-state to BR_D) (26), we assign τ_4 to the O-AR_{518} transition (S_oH/D_oH-S_oH/D_o). Thus, at negative voltage the O-intermediate is more populated and not a third M (M′) as suggested previously (16). The decay of O to AR_{518} is connected only to a small charge movement (27), which restrains it from direct electrical recording. The blue-light-induced negative current peak (Fig. 5 *F*) is interpreted in the usual way as photoisomerization and reprotonation of accumulated S_o (M-state) from the extracellular side (separate transition S_o-S_oH), whereas the reduction of the steady-state current is interpreted as a permanent two-photon reaction (green plus blue) (16). The finding that the apparent response to blue light in Fig. 5 *C* is voltage independent is important. This surprising observation means that the occupancy of the amount of deprotonated S_i and S_o (M-states) is voltage independent and that all rate-limiting, voltage-dependent steps of the photocycle are located downstream of S_o.

CONCLUSIONS

We draw the following conclusions:

1. AR is the first reported ion-pumping rhodopsin from a photosynthetic eukaryote.
2. AR is a light-driven H^+ pump similar to BR but with different sensitivities to voltage, pH_o, and pH_i.
3. The influence of the transmembrane voltage on the kinetic characteristics of ion-pumping rhodopsins obeys conventional, enzyme kinetic formalisms.
4. The intracellular H^+ donor group has a pK_a of 7.2, whereas the extracellular H^+ release group resembles a $pK_a > 9$.
5. In continuous light, M-like and O-like intermediates are accumulated, but only O is further enriched at negative voltage.

We thank Dr. Rolf Hagedorn for stimulating discussion.

This work was supported by the Deutsche Forschungsgemeinschaft (P.H.).

REFERENCES

1. Schilde, C. 1968. Rapid photoelectric effect in the alga *Acetabularia*. *Z. Naturforsch. B*. 23:1369–1376.
2. Gradmann, D. 1978. Green light (550 nm) inhibits electrogenic Cl^- pump in *Acetabularia* membrane by permeability increase for the carrier ion. *J. Membr. Biol*. 44:1–24.
3. Gradmann, D. 1984. Electrogenic chloride pump in the marine alga *Acetabularia*. *In* Chloride Transport Coupling in Biological Membranes and Epithelia. G. A. Gerencser, editor. Elsevier Biomedical Press, Amsterdam. 13–61.
4. Smahel, M., H. G. Klieber, and D. Gradmann. 1992. Vanadate-sensitive ATPase in the plasmalemma of Acetabularia: biochemical and kinetic characterization. *Planta*. 188:62–69.
5. Ikeda, M., R. Schmid, and D. Oesterhelt. 1990. A Cl^- translocating adenosinetriphosphatase in *Acetabularia acetabulum*. 1. Purification and characterization of a novel type of adenosinetriphosphatase that differs from chloroplast F1 adenosinetriphosphatase. *Biochemistry*. 29:2057–2065.
6. Schneider, S. U., M. B. Leible, and X. P. Yang. 1989. Strong homology between the small subunit of ribulose-1,5-bisphosphate carboxylase/oxygenase of two species of Acetabularia and the occurrence of unusual codon usage. *Mol. Gen. Genet*. 218:445–452.
7. Henry, I. M., M. D. Wilkinson, J. M. Hernandez, Z. Schwarz-Sommer, E. Grotewold, and D. F. Mandoli. 2004. Comparison of ESTs from juvenile and adult phases of the giant unicellular green alga *Acetabularia acetabulum*. *BMC Plant Biol*. 4:3–14.
8. Bieszke, J. A., E. N. Spudich, K. L. Scott, K. A. Borkovich, and J. L. Spudich. 1999. A eukaryotic protein, NOP-1, binds retinal to form an archaeal rhodopsin-like photochemically reactive pigment. *Biochemistry*. 38:14138–14145.
9. Beja, O., L. Aravind, E. V. Koonin, M. T. Suzuki, A. Hadd, L. P. Nguyen, S. Jovanovich, C. M. Gates, R. A. Feldman, J. L. Spudich, E. N. Spudich, and E. F. DeLong. 2000. Bacterial rhodopsin: evidence for a new type of phototrophy in the sea. *Science*. 289:1902–1906.
10. Bieszke, J. A., E. L. Braun, L. E. Bean, S. C. Kang, D. O. Natvig, and K. A. Borkovich. 1999. The nop-1 gene of Neurospora crassa encodes a seven transmembrane helix retinal-binding protein homologous to archaeal rhodopsins. *Proc. Natl. Acad. Sci. USA*. 96:8034–8039.
11. Waschuk, S. A., A. G. Bezerra, L. Shi, and L. S. Brown. 2005. *Leptosphaeria* rhodopsin: bacteriorhodopsin-like proton pump from a eukaryote. *Proc. Natl. Acad. Sci. USA*. 102:6879–6883.
12. Nagel, G., D. Ollig, M. Fuhrmann, S. Kateriya, A. M. Mustl, E. Bamberg, and P. Hegemann. 2002. Channelrhodopsin-1: a light-gated proton channel in green algae. *Science*. 296:2395–2398.
13. Nagel, G., T. Szellas, W. Huhn, S. Kateriya, N. Adeishvili, P. Berthold, D. Ollig, P. Hegemann, and E. Bamberg. 2003. Channelrhodopsin-2, a directly light-gated cation-selective membrane channel. *Proc. Natl. Acad. Sci. USA*. 100:13940–13945.

14. Luecke, H., B. Schobert, H. T. Richter, J. P. Cartailler, and J. K. Lanyi. 1999. Structural changes in bacteriorhodopsin during ion transport at 2 angstrom resolution. *Science*. 286:255–260.

15. Friedrich, T., S. Geibel, R. Kalmbach, I. Chizhov, K. Ataka, J. Heberle, M. Engelhard, and E. Bamberg. 2002. Proteorhodopsin is a light-driven proton pump with variable vectoriality. *J. Mol. Biol.* 321:821–838.

16. Geibel, S., T. Friedrich, P. Ormos, P. G. Wood, G. Nagel, and E. Bamberg. 2001. The voltage-dependent proton pumping in bacteriorhodopsin is characterized by optoelectric behavior. *Biophys. J.* 81:2059–2068.

17. Schweiger, H. G., P. Dehm, and S. Berger. 1977. Culture conditions for *Acetabularia*. *In* Progress in Acetabularia Research. C. L. F. Woodcock, editor. Academic Press, New !York. 319–330.

18. Müller, D. 1962. On year and lunar periodicity phenomenon in several brown algae. *Bot. Mar.* 4:140–155.

19. Kammann, M., J. Laufs, J. Schell, and B. Gronenborn. 1989. Rapid insertional mutagenesis of DNA by polymerase chain reaction (PCR). *Nucleic Acids Res.* 17:5404–5404.

20. Tyagi, R., R. Lai, and R. G. Duggleby. 2004. A new approach to 'megaprimer' polymerase chain reaction mutagenesis without an intermediate gel purification step. *BMC Biotechnol.* 4:2.

21. Grygorczyk, R., P. Hankebaier, W. Schwarz, and H. Passow. 1989. Measurement of erythroid band 3 protein-mediated anion transport in mRNA-injected oocytes of *Xenopus laevis*. *Methods Enzymol.* 173:453–466.

22. Stewart, A. K., M. N. Chernova, Y. Z. Kunes, and S. L. Alper. 2001. Regulation of AE2 anion exchanger by intracellular pH: critical regions of the NH(2)-terminal cytoplasmic domain. *Am. J. Physiol. Cell Physiol.* 281:C1344–C1354.

23. Gergely, C., C. Ganea, G. Groma, and G. Varo. 1993. Study of the photocycle and charge motions of the bacteriorhodopsin mutant D96N. *Biophys. J.* 65:2478–2483.

24. Garczarek, F., L. S. Brown, J. K. Lanyi, and K. Gerwert. 2005. Proton binding within a membrane protein by a protonated water cluster. *Proc. Natl. Acad. Sci. USA.* 102:3633–3638.

25. Brown, L. S., A. K. Dioumaev, R. Needleman, and J. K. Lanyi. 1998. Connectivity of the retinal Schiff base to Asp85 and Asp96 during the bacteriorhodopsin photocycle: the local-access model. *Biophys. J.* 75:1455–1465.

26. Richter, H. T., R. Needleman, H. Kandori, A. Maeda, and J. K. Lanyi. 1996. Relationship of retinal configuration and internal proton transfer at the end of the bacteriorhodopsin photocycle. *Biochemistry.* 35: 15461–15466.

27. Tóth-Boconádi, R., L. Keszthelyi, and W. Stoeckenius. 2003. Photoexcitation of the O-intermediate in bacteriorhodopsin mutant L93A. *Biophys. J.* 84:3848–3856.